Electronic Supplementary Material (ESI) for ChemComm.

Efficient biocatalytic C-H bond oxidation: an engineered heme-thiolate peroxygenase from a thermostable cytochrome P450

Supporting Information

Alecia R. Gee,[a] Isobella S. J. Stone, [a] Tegan P. Stockdale,[b] Tara, L. Pukala[a] James J. De Voss,[b] and Stephen G. Bell*[a]

[a.] School of Physics, Chemistry and Earth Sciences, University of Adelaide, Adelaide, SA 5005, Australia.

E-mail: stephen.bell@adelaide.edu.au

[b.] School of Chemistry and Molecular Biosciences, University of Queensland, Brisbane, Qld, 4072, Australia.

Contents

Experimental

General

General reagents and organics were purchased from Sigma-Aldrich, Tokyo Chemical Industry, Chem-Supply or Fluorochem. Isopropyl-β-D-thiogalactopyranoside (IPTG) and buffer components were obtained from Astral Scientific (Australia). The synthesis of [9,9,10,10-d_4]-dodecanoic acid has been described previously.[1]

UV-vis absorbance spectroscopy was performed on an Agilent Cary 60 spectrophotometer. Gas Chromatography-Mass Spectrometry was carried out on a Shimadzu GC-2010 with GC–MS-QP2010S detector. The interface and injection port temperatures were held at 280 and 250 °C, respectively. The column (DB5ms; 30 m x 0.25 mm x 0.25 μm) was held at 120 °C for 3 min, and the temperature was then increased to 240 ˚C at a rate of 7.5 °C min^{-1} and held at 240 °C for 6 min.

Protein expression and purification

Codon optimized versions of the genes encoding WT CYP119 and the CYP119 GALQEPG mutants were obtained in the plasmid, pET28b (Twist Bioscience; see below for details). This was transformed into *E. coli* BL21 (DE3) competent cells and grown on an LB plate in the presence of kanamycin (30 μg/mL).[27, 44] A single colony was added to 500 mL of LB media containing trace elements solution ($CaCl_2$, $ZnSO_4.7H_2O$, $MnSO_4.H_2O$, Na_2-EDTA, $FeCl_3.6H_2O$, $CuSO_4.5H_2O$, and $CoCl_2.6H_2O$) in the presence of antibiotic and incubated at 37 °C at 85 rpm. After 10 h incubation 0.02 % v/v benzyl alcohol and 2 % v/v ethanol were added and after an additional 30 min 100 μM isopropyl ß-D-1-thiogalactopyranoside (IPTG) was used to induce protein production.

Cells were harvested after 24 h by centrifugation (5000 *g*, 10 min, 4 °C) and resuspended in 200 mL 50 mM Tris buffer (pH 8.0 containing 200 μL 2-mercaptoethanol, 2 mL PMSF (10 mM) and 10% glycerol). The cells were lysed by sonication on ice for 30 cycles (20 s on, 40 s off) and cell debris was removed by centrifugation (37,000 *g*, 20 min, 4 °C). The supernatant was loaded onto a His-trap column (GE Healthcare) equilibrated with sample loading buffer (20 mM sodium phosphate, 20 mM imidazole, 0.5 M NaCl, pH 8.0). The column was washed with 5 column volumes of the sample loading buffer before elution of the His-tagged protein with sample elution buffer (20 mM sodium phosphate buffer, pH 8.0, 0.5 M NaCl and 500 mM imidazole). The cytochrome P450 containing fractions were concentrated by ultrafiltration (10 kDa exclusion membrane) and afterwards the protein was loaded to a Sephadex G-25 medium grain column (250 mm x 40 mm; Cytiva) to desalt using 50 mM Tris buffer, pH 8.0. The protein was concentrated by ultrafiltration and further purified by anion-exchange chromatography using a Source 15Q column (XK26, 80 x 30 mm; Cytiva)**,** eluting the protein with a gradient (0-250 mM KCl in 50 mM Tris buffer, pH 8.0). The protein was concentrated by ultrafiltration and an equivalent volume of 80% glycerol was added to the protein and filter sterilized before storage at -20 °C. Glycerol was removed from the enzyme before subsequent experiments using a PD-10 desalting column (Cytiva) and eluting into 50 mM Tris buffer, pH 8.0.

CYP119 characterisation

CO-binding analysis

Solutions of CYP119 WT and mutant GALQEPG (10 – 50 μM) in 500 μL Tris-HCl buffer (50 mM, pH 8.0) were analysed via UV-Vis spectroscopy between 700 and 250 nm. A couple grains of sodium dithionate were added to the solution to reduce the heme of the P450 and were again analysed via UV-Vis spectroscopy. CO was then bubbled through 400

μL of Tris-HCl buffer (50 mM, pH 8.0) for approximately 10 s. This CO enriched buffer was added to each of the CYP119 solutions for coordination of CO to the reduced heme and the spectra were again recorded. The molar absorptivity of CYP119 WT was calculated to be ε_{415} = 121 $mM^{-1}cm^{-1}$ using the differential spectra from Fe-(II)-CO against unbound Fe(II) where $\varepsilon_{450 - 490}$ = 91 $mM^{-1}cm^{-1}$ as per the Omura and Sato method.[2]

Spin state shift analysis

CYP119 WT and GALQEPG solutions (3 μM in 600 μL) in Tris-HCl buffer (50 mM, pH 8.0) were analysed via UV-Vis spectroscopy from 250 to 700 nm. Dodecanoic acid (from a 100 mM stock solution in EtOH) was added to the solutions in 1 μL aliquots and the spectra were recorded until no further shift in the Soret peak was detected.

Activity assays

Heme bleaching assay

A 600 μL aliquot of CYP119 WT and GALQEPG mutant (3 μM) in Tris buffer (50 mM, pH 8.0) was used to baseline the spectrophotometer. Dodecanoic acid (1 mM) and H_2O_2 (60 mM) were added, and the UV-vis spectrum was recorded. Heme prosthetic group destruction was monitored by recording UV-vis spectra at 2 min intervals.

Peroxygenase assays

The peroxygenase oxidation assays for the WT enzyme and GALQEPG variant of CYP119 were run in a total volume of 600 μL consisting of Tris buffer (50 mM, pH 8.0), 3 μM enzyme and 1 mM substrate. The reactions were started by addition of H_2O_2 (50 mM) and incubated for 2-4 hrs.

To determine the rate of fatty acid oxidation, reactions were undertaken with 1 μM of the GALQEPG variant of CYP119 and 100 μM tetradecanoic acid at 30 °C and 70 °C

and 500 µM dodecanoic acid at 70 °C . The reactions were started by addition of 20 mM H_2O_2 and incubated for 5 minutes. The reaction was quenched by adding catalase (see Figure S24 and Figure S25).

Product analysis

After reactions were completed, 595 µL of the reaction mixture was mixed with 5 µL of an internal standard solution (octanoic acid, 20 mM stock solution in EtOH). These mixtures were extracted with 3 x 400 µL of ethyl acetate and dried with anhydrous $MgSO_4$. The organic solvent was then removed under a stream of dinitrogen gas and the residue was dissolved in anhydrous acetonitrile. Bis(trimethylsilyl)trifluoroacetamide (BSTFA) with 1% trimethylchlorosilane (TMCS), 15 µL was added to the acetonitrile to derivatize the substrate and metabolites. After leaving these samples for 2 hours at 37 °C they were used directly for GC-MS analysis. Products were initially identified by the GC-MS fragmentation patterns of the derivatized hydroxylated fatty acids (See Figures S8 to S23). It was assumed that isomeric products would give comparable detector responses. All reactions were performed in duplicate.

Synthesis of 9-(oxiran-2-yl)nonanoic acid

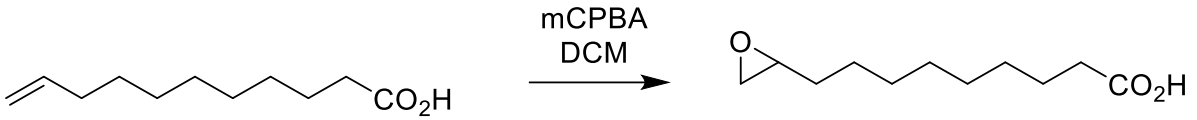

A solution of 10-undecenoic acid (202 mg, 1.10 mmol) in DCM (3 mL) was cooled to 0˚C and *meta*-chloroperbenzoic acid (209 mg, 1.21 mmol) was added portion-wise. The reaction was allowed to come to room temperature and stirred for 4.5 h. The reaction was quenched by addition of distilled water (3 mL), diluted with DCM (5 mL) and partitioned. The aqueous layer was further extracted with DCM (5 mL), the combined organic extracts were washed with brine (5 mL), dried over magnesium sulfate, filtered and concentrated *in vacuo*. The crude residue

was purified by flash column chromatography (silica gel, 10-20% ethyl acetate in petroleum spirits 40-60) to yield the the epoxide as a white solid (87.6 mg, 0.44 mmol, 40%).

^{1}H NMR (500 MHz, $CDCl_3$) δ 1.25 – 1.37 (m, 10H), 1.39 – 1.49 (m, 1H), 1.49 – 1.57 (m, 2H), 1.63 (p, *J* = 7.3 Hz, 2H), 2.35 (t, *J* = 7.5 Hz, 2H), 2.47 (dd, *J* = 5.0, 2.8 Hz, 1H), 2.75 (dd, *J* = 5.0, 4.0 Hz, 1H), 2.91 (tdd, *J* = 5.5, 4.0, 2.7 Hz, 1H).

^{13}C NMR (126 MHz, $CDCl_3$) δ 24.6, 25.9, 29.0, 29.1, 29.3, 29.3, 32.4, 33.8, 47.1, 52.4, 178.7.

HRMS-ESI *(m/z)*: $[M+Na]^+$ calcd for $C_{11}H_{20}O_3Na$, 223.1305; Found: 223.3012.

Kinetic isotope effect calculations

A previously synthesised deuterated dodecanoic substrate ([9,9,10,10-d_4]-dodecanoic acid) was used as a substrate to calculate the kinetic isotopic effect.[1] To calculate KIE, the integration of the chromatographic peaks corresponding to each of the labelled sites was first measured, as well as the sum of the integrated peaks for the unlabelled sites.[3]

To calculate the KIE for [9,9,10,10-d_4] labelled dodecanoic acid deuterated at ω – 2 and ω – 3 positions, we divide the ratio of products at deuterated site A^D and products at non-deuterated site B^H (A^D:B^H) by the observed ratio of unlabelled material (A^H:B^H) which provides a ratio of rate constants as follows:

$$(A^D/B^H)/(A^H/B^H) = (k_1{}^D/k_2{}^H)/(k_1{}^H/k_2{}^H)$$

This cancels to

$$k_1{}^D/k_1{}^H$$

which is by definition the kinetic isotope effect for a compound deuterated at A.

Gene synthesis

The following codon optimized sequences were obtained from Twist Bioscience and cloned into the pET28 vector between the Nco I and Xho I restriction sites. The NcoI site (CCATGG) contains the start codon. A 6xHis tag and TEV cleavage sequence was incorporated at the N-terminus (bold) a Nde I restriction site (underlined) followed by the gene of interest. This was followed by two stop codons (bold and italics) and Kpn I and Hind III restriction sites (underlined). The codons for the GALQEPG mutations are highlighted in yellow.

WT CYP119

GTGGCTCCAGCCATCACCATCACCATCACAGCAGCGGCGAAAACCTGTACTTCCAGGGC<u>CAT</u>
<u>ATG</u>TATGATTGGTTTTCAGAGATGCGGAAAAAGGACCCAGTGTATTATGATGGTAATATTTGGCAG
GTTTTCTCATACCGCTATACTAAGGAGGTACTTAATAACTTCAGCAAGTTTAGTTCTGACCTCACAG
GCTACCACGAGCGTTTAGAGGATCTGCGTAATGGGAAGATCCGTTTTGATATTCCGACGCGATACA
CAATGCTTACATCTGATCCACCGTTACATGATGAGCTGAGAAGCATGTCCGCAGACATTTTTAGTC
CGCAGAAGCTTCAGACATTGGAAACCTTCATTAGAGAAACTACCCGTAGCCTCCTTGATTCAATTG
ATCCCCGTGAAGACGACATAGTCAAAAAGTTGGCAGTTCCTCTTCCAATCATAGTCATCAGTAAAA
TATTGGGTCTGCCGATCGAAGATAAGGAAAAATTCAAAGAATGGAGCGACCTTGTGGCCTTTCGTC
TTGGCAAACCTGGTGAGATATTCGAGCTGGGTAAAAAGTACCTGGAGTTAATCGGCTACGTAAAA
GATCATCTTAATAGTGGTACCGAGGTTGTGTCTCGGGTTGTTAATTCTAATCTTAGCGATATCGAG
AAATTGGGCTATATAATATTGCTCTTGATTGCGGGCAATGAAACAACGACCAACCTGATCAGTAAC
AGCGTTATCGATTTCACACGATTTAATTTATGGCAGCGGATCCGGGAGGAAAATCTTTACCTGAAG
GCAATCGAGGAAGCACTTCGCTATTCTCCCCCAGTGATGCGTACCGTTCGCAAGACCAAAGAGAG
AGTGAAACTGGGGGACCAAACGATTGAAGAAGGGGAGTATGTCCGTGTTTGGATTGCCTCTGCGA
ACCGTGATGAAGAGGTTTTTCACGACGGTGAAAAATTTATCCCTGATCGCAATCCAAACCCACATC
TCAGCTTTGGCTCGGGCATACATTTGTGCCTGGGCGCGCCCCTGGCTCGTCTCGAAGCGAGAATCG
CCATAGAGGAGTTTTCAAAGCGGTTTCGTCACATAGAGATTCTTGACACGGAGAAAGTACCCAAT
GAGGTGCTGAATGGCTATAAGCGCCTCGTCGTTCGCTTAAAAAGCAACGAA***TAATAG***<u>GGTACCAA</u>
<u>GCTT</u>

CYP119 GALQEPG mutant

GTGGCTCCAGCCATCACCATCACCATCACAGCAGCGGCGAAAACCTGTACTTCCAGGGC<u>CAT</u>
<u>ATG</u>TATGACTGGTTCTCTGAAATGCGAAAAAAGGACCCAGTTTACTATGACGGCAACATATGGCA
AGTCTTTAGTTACCGTTACACGAAGGAAGTTTTGAATAACTTTTCAAAATTCTCTAGTGATCTGACC
GGGTATCATGAGCGTCTTGAAGACCTGAGAAATGGCAAGATCCGTTTCGACATACCTACGCGTTAC
ACTATGTTAACAAGTGACCCCCCATTACATGATGAGCTGCGTTCTATGTCTGCGGATATCTTTTCAC
CCCAGAAACTGCAGACCCTGGAGACCTTCATTCGCGAAACTACTAGAAGTTTGTTAGACAGCATTG
ACCCTCGAGAGGACGATATTGTTAAAAAGCTGGCGGTGCCACTTCCAATTATCGTCATCTCTAAAA
TCTTGGGGCTTCCGATTGAAGATAAAGAGAAATTCAAGGAATGGTCTGACCTTGTGGCATTTCGGT
TAGGAAAACCCGGCGAGATATTTGAGCTGGGGAAGAAGTATCTGGAATTAATAGGGTACGTGAAA
GATCATCTGAATTCTGGAACGGAAGTCGTTTCTCGGGTCGTAAACTCCAATCTTAGCGACATTGAG
AAACTGGGGTATATAATCCTTCTGCTTATAGGTGCTTTACAAGAGCCTGGCAATTTAATCTCTAATT
CCGTGATCGATTTTACACGTTTTAATCTGTGGCAGCGTATTCGTGAAGAGAACCTTTATCTGAAAG
CCATCGAAGAAGCTCTGCGGTATTCTCCGCCGGTGATGCGTACCGTCCGCAAAACTAAGGAACGC
GTTAAGCTGGGTGATCAAACTATTGAGGAAGGGGAATACGTGCGGGTCTGGATAGCCTCTGCGAA
CCGTGATGAAGAGGTCTTTCATGACGGAGAGAAGTTCATCCCTGATAGAAATCCGAATCCTCACTT
ATCTTTCGGCTCTGGAATTCATCTCTGCCTCGGGGCGCCCTTGGCCCGGTTAGAAGCAAGAATCGC
TATAGAGGAATTTTCAAAACGCTTTCGGCATATTGAAATCTTAGATACGGAAAAAGTCCCCAACGA
GGTATTGAATGGATATAAACGCCTGGTTGTACGGCTTAAGTCCAACGAA***TAATAG***<u>GGTACCAAGCT</u>
<u>T</u>

Tables

Table S1 The product distribution of dodecanoic acid oxidation by the GALQEPG peroxygenase variant of CYP119 by comparison to wild type at room temperature.

Metabolite	dodecanoic acid	
	WT	GALQEPG
desat	0.1 ± 0.18	0.4 ± 0.00
ω	1.0 ± 0.73	0.5 ± 0.05
ω-1	31.2 ± 0.20	26.9 ± 0.24
ω-2	61.1 ± 0.12	63.7 ± 0.34
ω-3	2.0 ± 0.45	2.3 ± 0.08
ω-1 ketone	3.3 ± 0.70	1.5 ± 0.24
ω-2 ketone	1.2 ± 0.34	4.6 ± 0.48

Table S2 The product distribution of fatty acid oxidation by the GALQEPG peroxygenase variant of CYP119 at room temperature.

	C10	C11	C12	C13	C14	d_4-dodecanoic acid
desaturation	6.2 ± 0.37	1.7 ± 0.03	0.3 ± 0.01	0.3 ± 0.03	-	-
ω	4.1 ± 0.31	0.5 ± 0.07	0.4 ± 0.07	0.2 ± 0.03	-	0.7 ± 0.01
ω-1	73.2 ± 0.94	76.6 ± 0.24	26.3 ± 0.12	44.5 ± 0.37	31.5 ± 0.49	63.1 ± 0.38
ω-2	16.5 ± 0.26	16.4 ± 0.12	65.3 ± 0.32	33.6 ± 0.09	59.0 ± 0.79	26.7 ± 0.05
ω-3	-	0.6 ± 0.07	2.7 ± 0.06	18.1 ± 0.18	6.7 ± 0.11	0.7 ± 0.04
ω-4	-	-	-	0.9 ± 0.02	2.9 ± 0.20	-
ω-1 ketone	-	3.4 ± 0.09	1.2 ± 0.07	1.1 ± 0.00	-	6.6 ± 0.17
ω-2 ketone	-	0.9 ± 0.07	3.8 ± 0.16	0.9 ± 0.08	-	2.1 ± 0.13
ω-3 ketone	-	-	-	0.3 ± 0.01	-	-

Table S3 The product distribution of lauric acid oxidation by the GALQEPG peroxygenase variant of CYP119 at varying temperatures (°C).

	RT		50	70	80		90
	WT	GALQEPG	GALQEPG	GALQEPG	WT	GALQEPG	GALQEPG
desat	0.1 ± 0.18	0.4 ± 0.00	-	-	1.2 ± 0.09	0.3 ± 0.01	-
ω	1.0 ± 0.73	0.5 ± 0.05	0.2 ± 0.02	0.6 ± 0.06	2.1 ± 1.40	0.9 ± 0.02	0.8 ± 0.07
ω-1	31.2 ± 0.20	26.9 ± 0.24	21.9 ± 0.10	29.2 ± 1.26	44.5 ± 1.55	34.4 ± 0.32	34.7 ± 0.14
ω-2	61.1 ± 0.12	63.7 ± 0.34	45.8 ± 0.22	50.3 ± 0.98	43.7 ± 0.58	55.6 ± 0.26	56.7 ± 0.61
ω-3	2.0 ± 0.45	2.3 ± 0.08	2.1 ± 0.10	2.7 ± 0.19	3.7 ± 0.49	3.0 ± 0.02	2.9 ± 0.05
ω-1 ketone	3.3 ± 0.70	1.5 ± 0.24	8.3 ± 0.07	5.4 ± 0.80	4.8 ± 0.15	2.0 ± 0.05	1.6 ± 0.28
ω-2 ketone	1.2 ± 0.34	4.6 ± 0.48	21.7 ± 0.17	11.8 ± 1.70	-	3.7 ± 0.00	3.4 ± 0.35

Figures

Spin state shifts

CYP119 WT

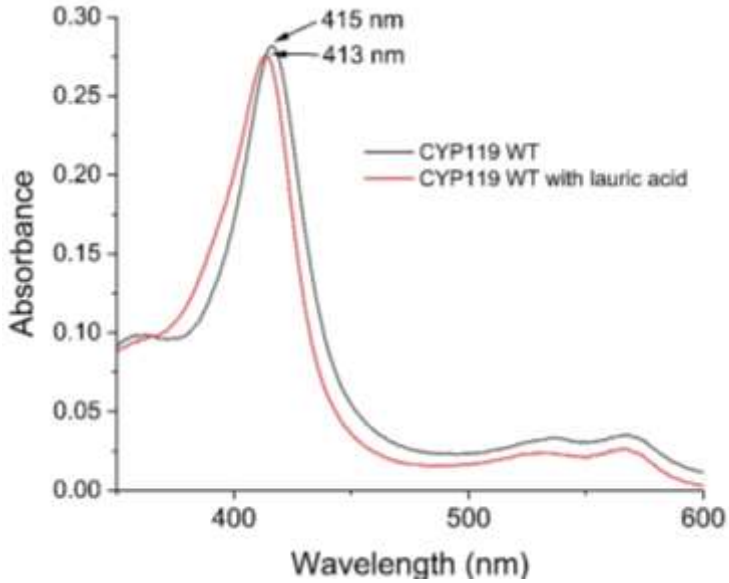

Figure S1 UV-vis absorbance spectra of spin-state shift for wildtype CYP119. In black, the resting state (Fe^{3+}) is shown with a Soret peak at 415 nm. Upon binding of the substrate (lauric acid), a slight blue shift is observed with a Soret peak of 413 nm (shown in red).

CYP119 GALQEPG

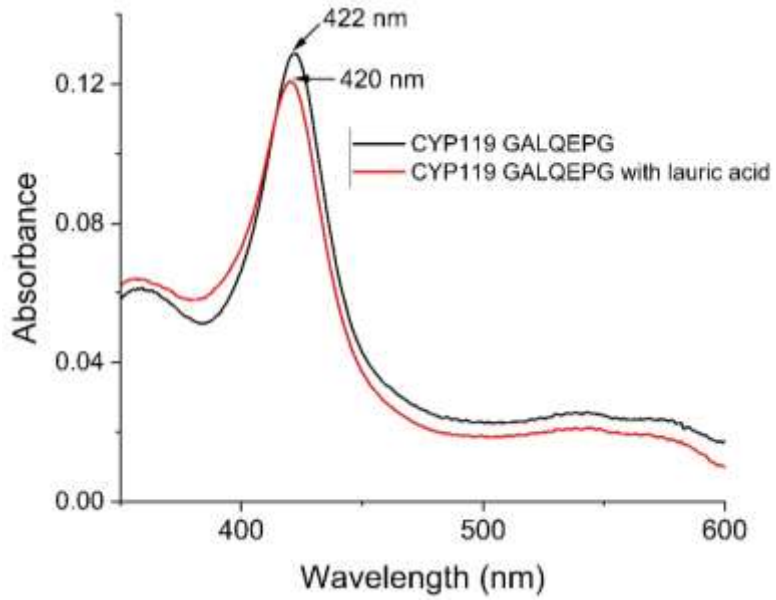

Figure S2 UV-vis absorbance spectra of spin-state shift for CYP119 GALQEPG. In black, the resting state (Fe^{3+}) is shown with a Soret peak at 422 nm. Upon binding of the substrate (lauric acid), a slight blue shift is observed with a Soret peak of 420 nm (shown in red).

CO spectra

CYP119 WT

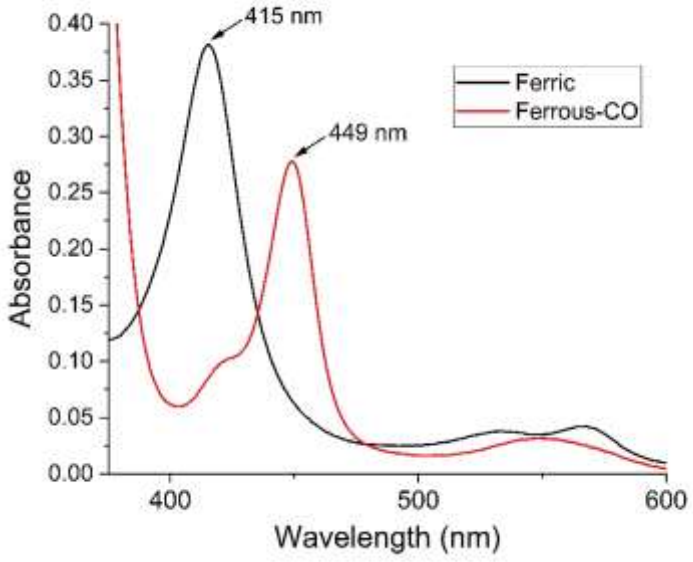

Figure S3 UV-vis absorbance of resting ferric state of CYP119 WT with observed Soret peak at 415 nm. CO-bound ferrous state is shown in red, whereby a near complete red shift to 449 nm occurs upon the binding of CO.

Using the same method as above results in an incomplete shift of the Soret of the ferrous-CO spectrum of CYP119-perox7 (Figure 2). This is in agreement with studies on similar mutated P450 enzymes. These mutants, which add an acidic residue close to the heme can interact strongly with the heme aqua ligand.[1] This results in the reduction of these enzymes being more challenging (slow) than in the WT P450 and modification of the ferrous-CO environment and therefore spectrum (see references 11).

Heme bleaching

CYP119 GALQEPG without substrate

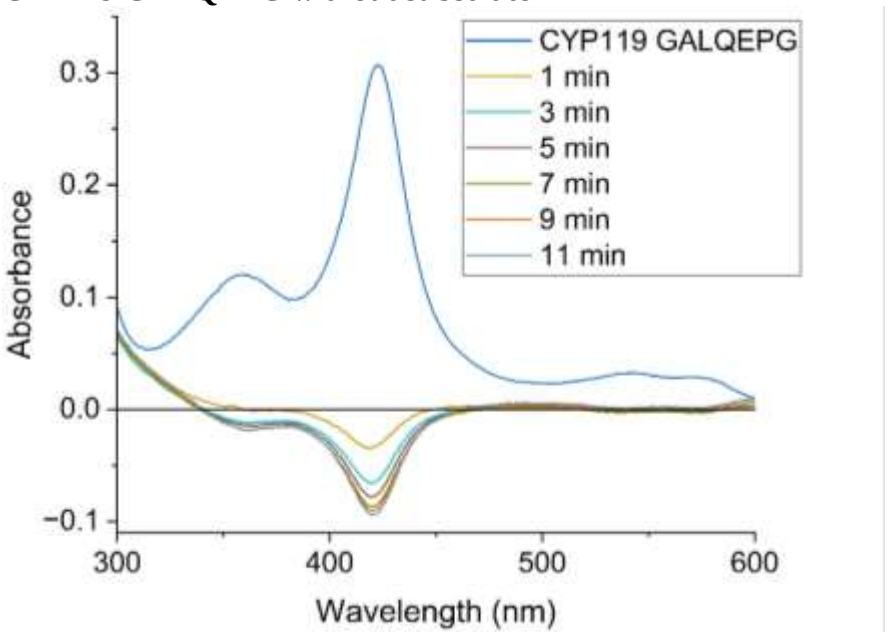

Figure S4 Heme bleaching assay of the CYP119 GALQEPG mutant (3 μM) in the presence of 60 mM H_2O_2 in the absence of substrate. The heme was partially bleached within 11 minutes where further loss of the Soret peak was minimal.

CYP119 GALQEPG with substrate

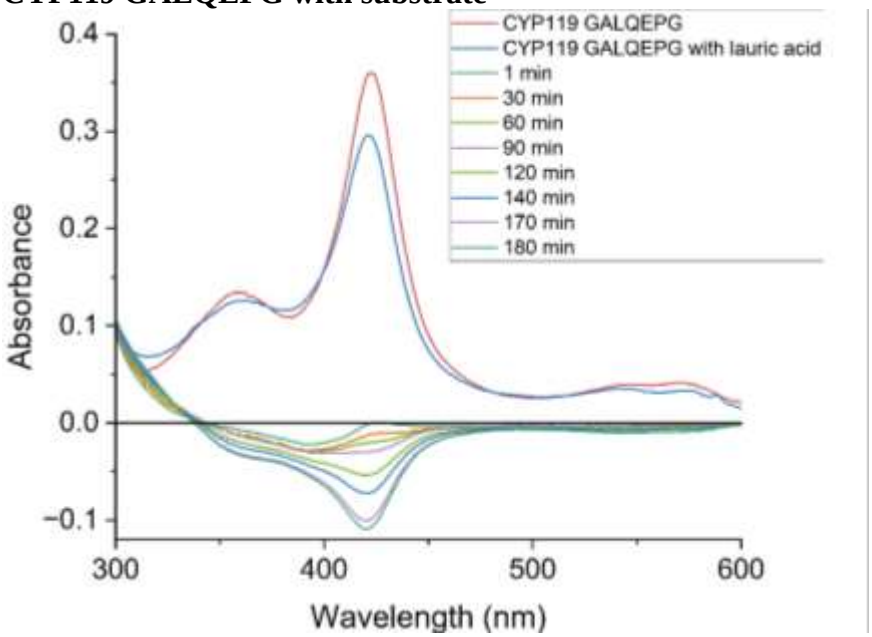

Figure S5 Heme bleaching assay of CYP119 GALQEPG done (3 μM) in the presence of 1 mM lauric acid and 60 mM H_2O_2. Heme bleaching was slower, with very little occurring over the first 30 minutes. After this time it accelerated but took 3 hours to achieve the similar levels of heme Soret band reduction as was seen in the absence of substrate.

CYP119 WT without substrate

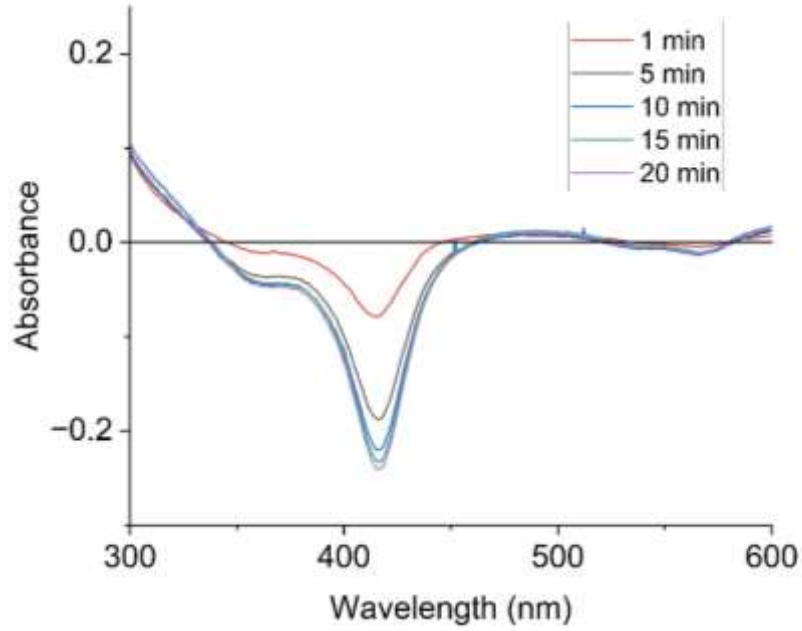

Figure S6 Heme bleaching assay of CYP119 WT (3 μM) done in the presence of 60 mM H_2O_2 and no substrate. The heme was largely degraded within 15 minutes where further loss of the Soret peak was no longer seen.

CYP119 WT with substrate

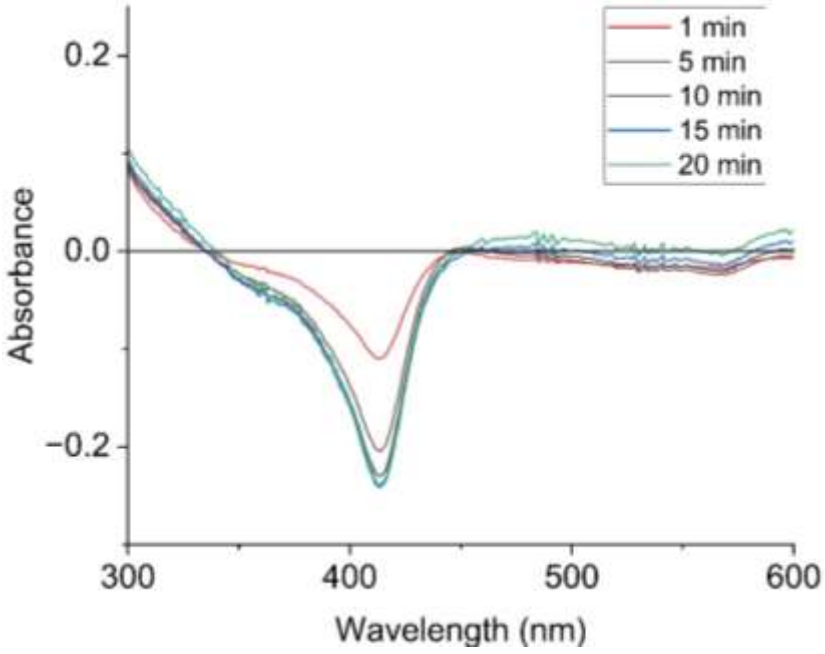

Figure S7 Heme bleaching assay of CYP119 WT (3 μM) done in the presence of 1 mM lauric acid and 60 mM H_2O_2. Heme degradation was comparable to the test with no substrate, with near complete degradation occurring after 15 minutes.

GCMS data for H_2O_2 turnovers with lauric acid

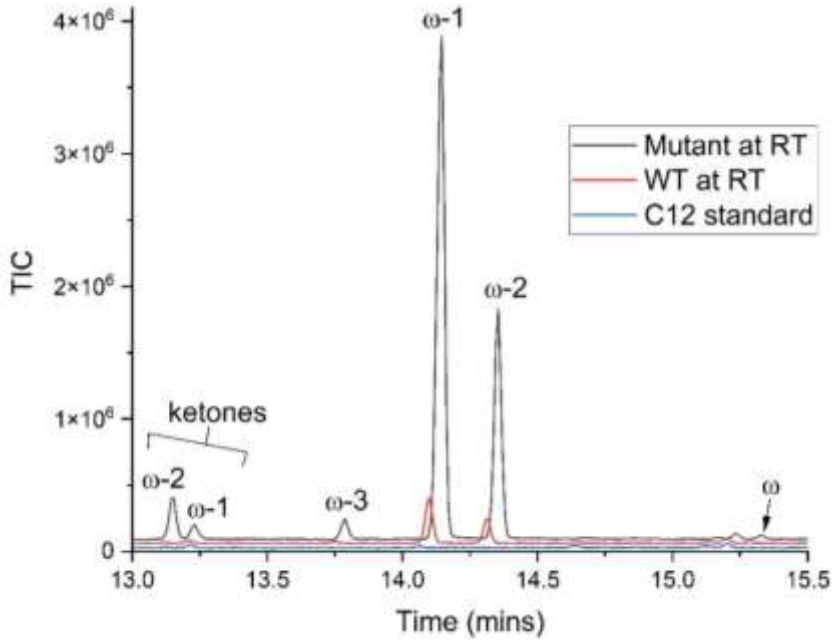

Figure S8 Chromatogram collected from GCMS shows products from H_2O_2 turnovers in the presence of CYP119 GALQEPG versus WT, 1 mM lauric acid and 50 mM H_2O_2 analysed at room temperature.

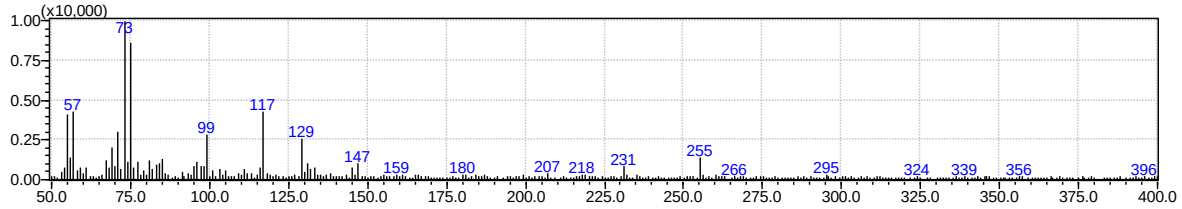

Desaturation of dodecanoic acid

11-dodecenoic acid. R.T. 10.183 to 10.267**.** Observed m/z = 255 (parent ion – 15; -Me) vs expected m/z = 270. See Figure S10.

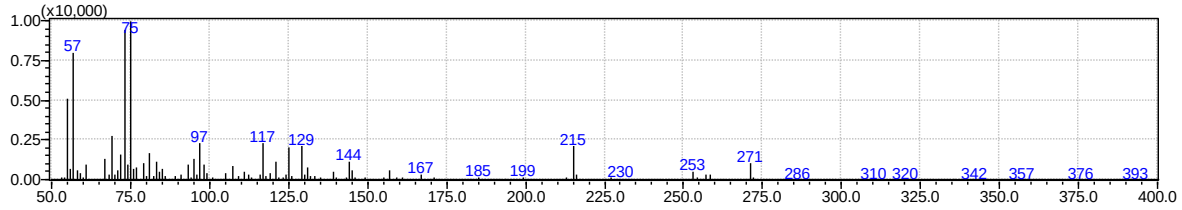

10-oxododecanoic acid

Dodecanoic acid ketone derivative at ω – 1. RT: 13.092 to 13.142. Observed m/z = 286 and 271 (- 15; -Me) vs expected 286; fragment at 215.

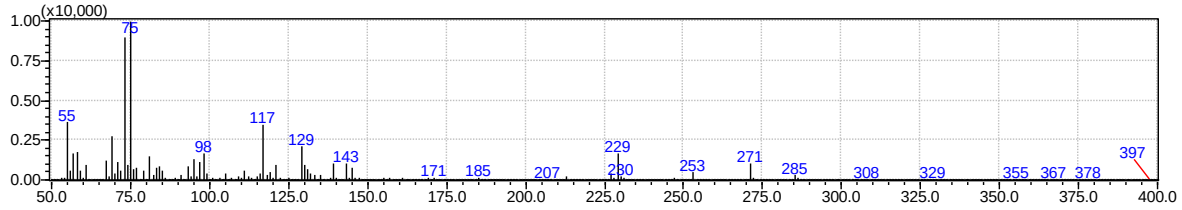

11-oxododecanoic acid

Dodecanoic acid ketone derivative at ω - 2. RT: 13.175 to 13.217. Observed m/z = 286 and 271 (- 15; -Me) vs expected 286; fragment at 229.

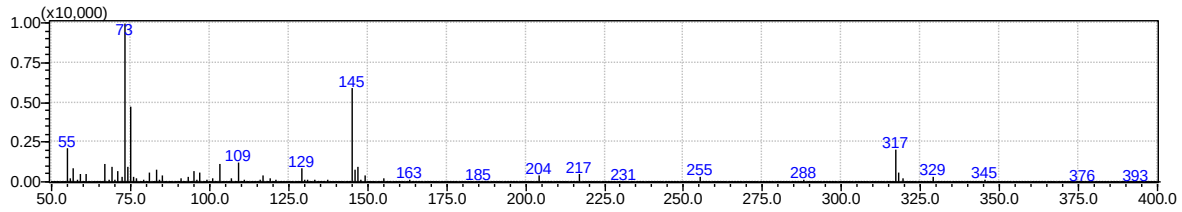

9-hydroxydodecanoic acid

Dodecanoic acid hydroxy derivative at ω - 3. RT: 13.725 to 13.792. Observed m/z = 345 (- 15; -Me) vs expected 360; fragments at 145 and 317.

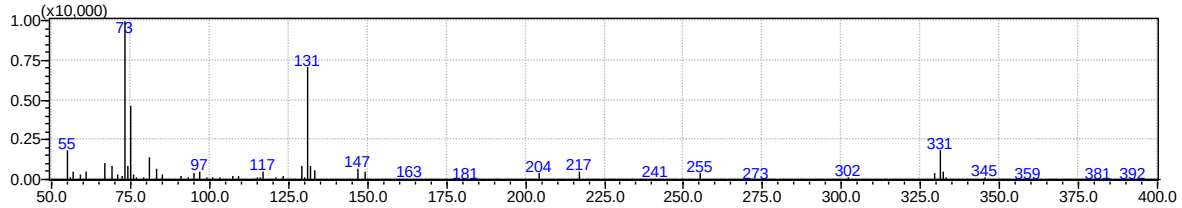

10-hydroxydodecanoic acid

Dodecanoic acid hydroxy derivative at ω - 2. RT: 14.058 to 14.150. Observed m/z = 345 (- 15; -Me) vs expected 360; fragments at 131 and 331.

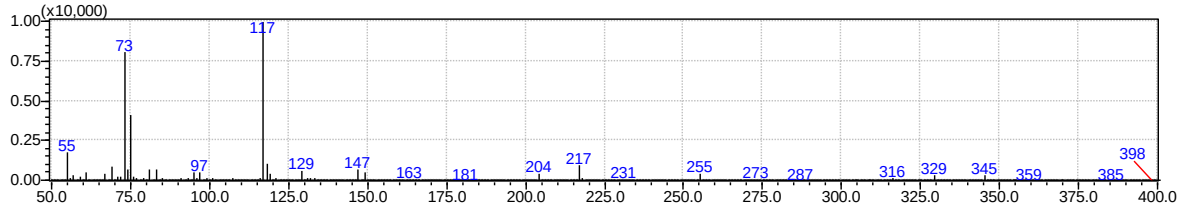

11-hydroxydodecanoic acid

Dodecanoic acid hydroxy derivative at ω - 1. RT: 14.275 to 14.367. Observed m/z = 345 (- 15; -Me) vs expected 360; fragments at 117 and 345.

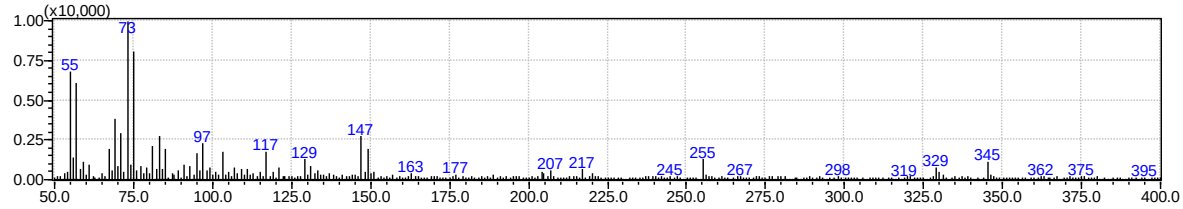

12-hydroxydodecanoic acid

Dodecanoic acid hydroxy derivative at ω. RT: 15.275 to 15.317. Observed m/z = 345 (- 15; -Me) vs expected 360; fragment at 103.

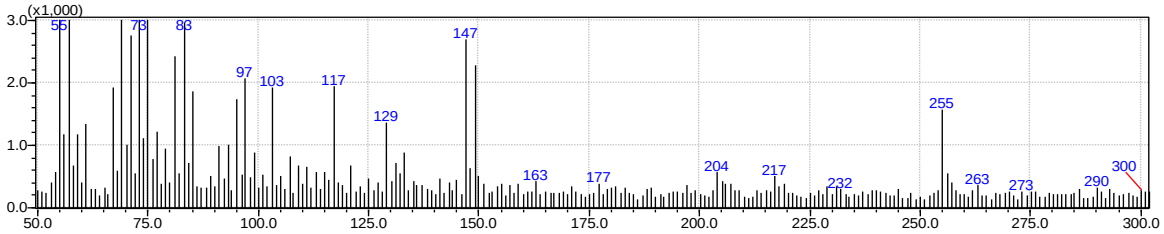

12-hydroxydodecanoic acid

Zoom in to show fragment at 103.

Figure S9 Mass spectra associated with chromatogram from Figure S8 for the reaction of lauric acid with CYP119 GALQEPG mutant in the presence of H_2O_2.

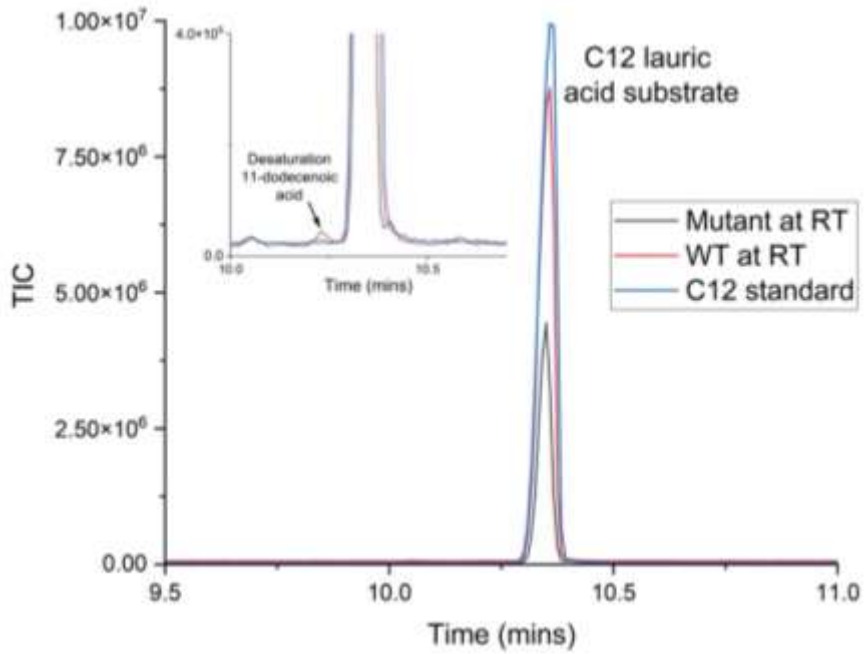

Figure S10 Chromatogram collected from GCMS of H_2O_2 turnovers in the presence of CYP119 GALQEPG, 1 mM lauric acid and 50 mM H_2O_2 analysed at room temperature. Substrate peak and desaturation product, 11-dodecenoic acid are shown.

Comparison of metabolite distribution for C10 – C14 fatty acid substrates

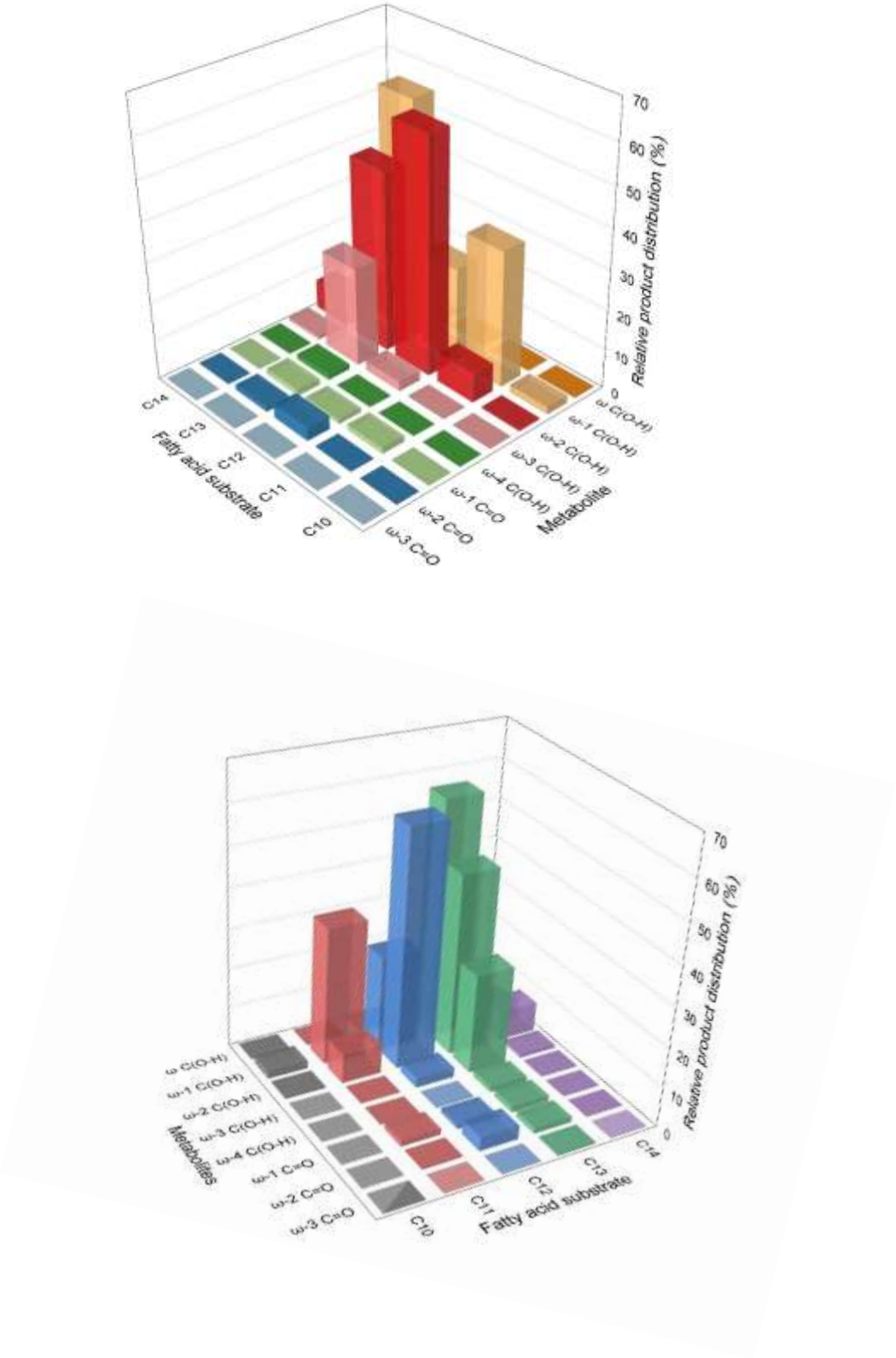

Figure S11 Relative product distribution of H_2O_2 turnovers with CYP119 GALQEPG and varying carbon chain length fatty acids (C10 to C14).

GCMS data for H_2O_2 turnovers for other fatty acids

10-undecenoic acid

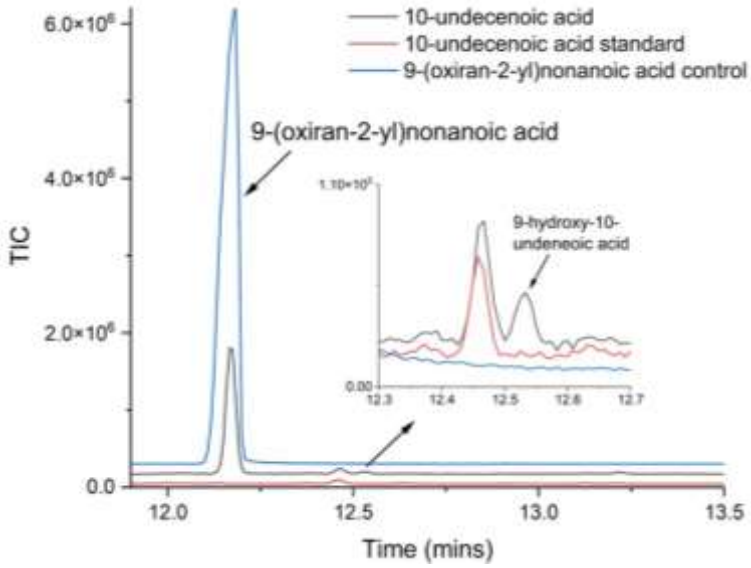

Figure S12 Chromatogram collected from GCMS data shows products from H_2O_2 turnovers in the presence of CYP119 GALQEPG, 1 mM 10-undecenoic acid and 50 mM H_2O_2.

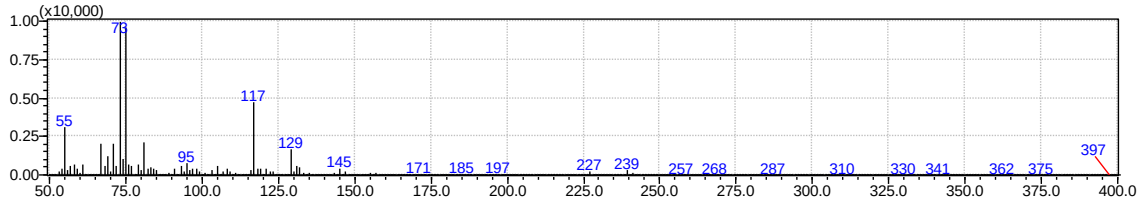

9-(oxiran-2-yl)nonanoic acid. R.T: 12.125 to 12.208. Observed m/z = 257 (- 15; -Me) vs expected m/z = 272.

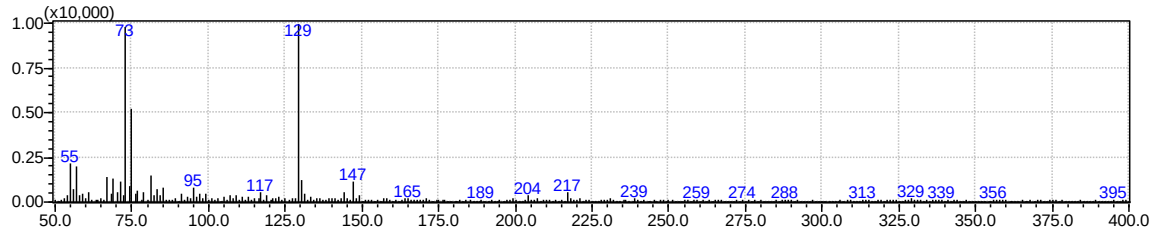

9-hydroxy-10-undecenoic acid. R.T: 12.492 to 12.533. Observed m/z = 329 (- 15; -Me) vs expected m/z = 344. Identified as the same product generated with CYP102 enzymes and confirmed by synthesis of the crude product (see below).[1]

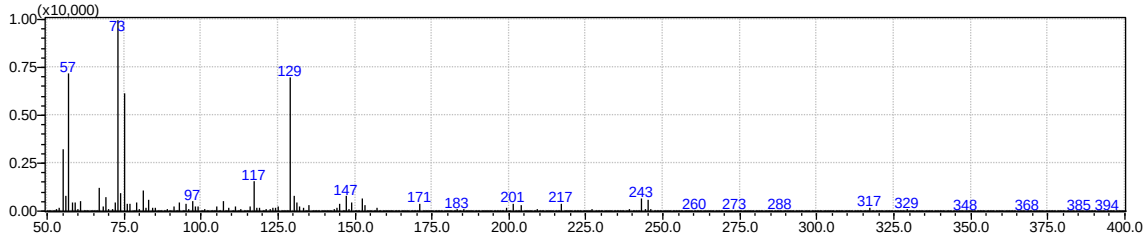

9-hydroxy-10-undecenoic acid from crude material; synthesised using a literature method.[4]

Figure S13 Mass spectra associated with chromatogram from Figure S12 for the reaction of 10-undecenoic acid with CYP119 GALQEPG mutant in the presence of H_2O_2.

Decanoic acid - C10

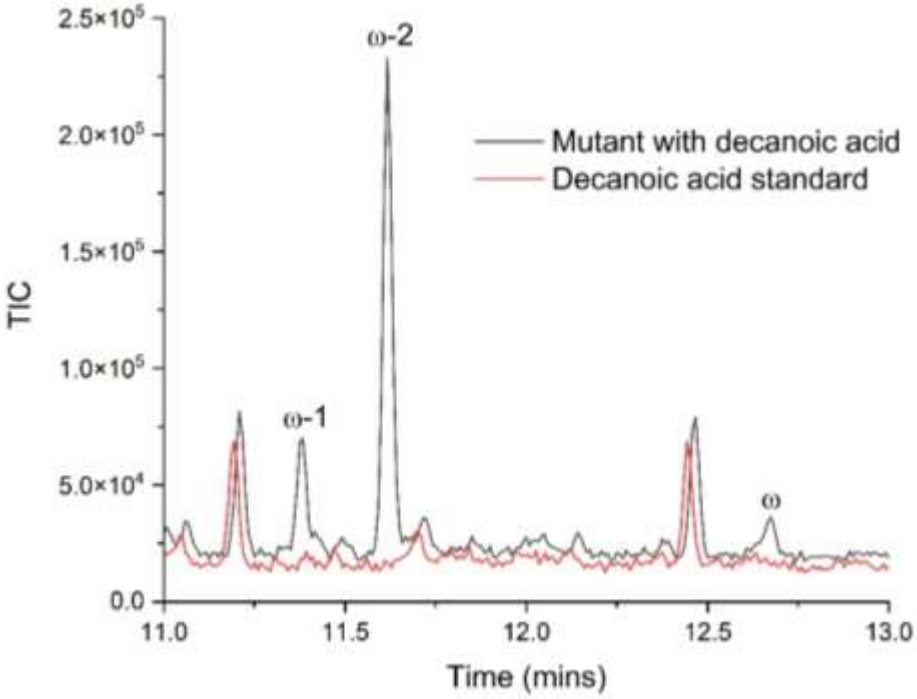

Figure S14 Chromatogram collected from GCMS shows products from H_2O_2 turnovers in the presence of CYP119 GALQEPG, 1 mM decanoic acid and 50 mM H_2O_2.

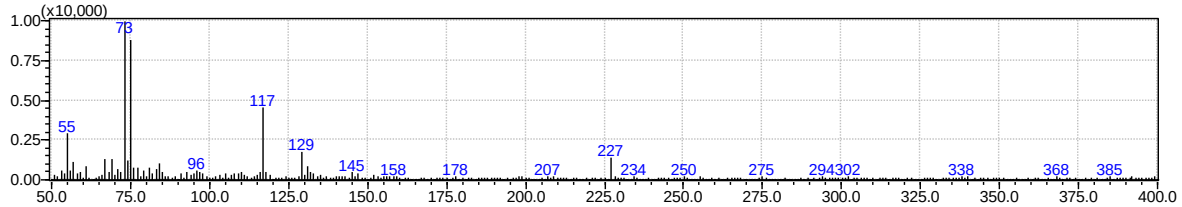

Desaturation of decanoic acid

9-decenoic acid. R.T. 7.008 to 7.092**.** Observed m/z = 227 (- 15; -Me) vs expected m/z = 242.

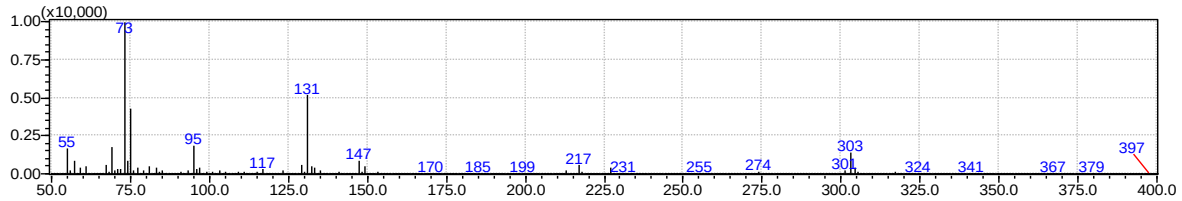

8-hydroxydecanoic acid

Decanoic acid hydroxy derivative at ω - 2. RT: 11.350 to 11.400. Observed m/z = 317 (- 15; -Me) vs expected 332; fragments at 131 and 303.

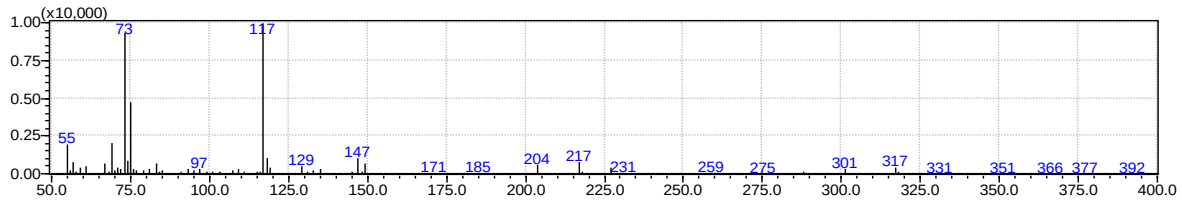

9-hydroxydecanoic acid

Decanoic acid hydroxy derivative at ω - 1. RT: 11.583 to 11.650. Observed m/z = 317 (- 15; -Me) vs expected 332; fragments at 117 and 317.

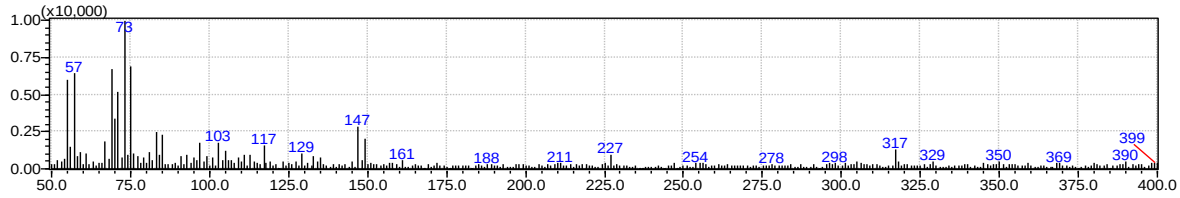

10-hydroxydecanoic acid

Decanoic acid hydroxy derivative at ω. RT: 12.650 to 12.683. Observed m/z = 317 (- 15; -Me) vs expected 332; fragment at 103.

Figure S15 Mass spectra associated with chromatogram from Figure S14 for the reaction of decanoic acid with CYP119 GALQEPG mutant in the presence of H_2O_2.

Undecanoic acid - C11

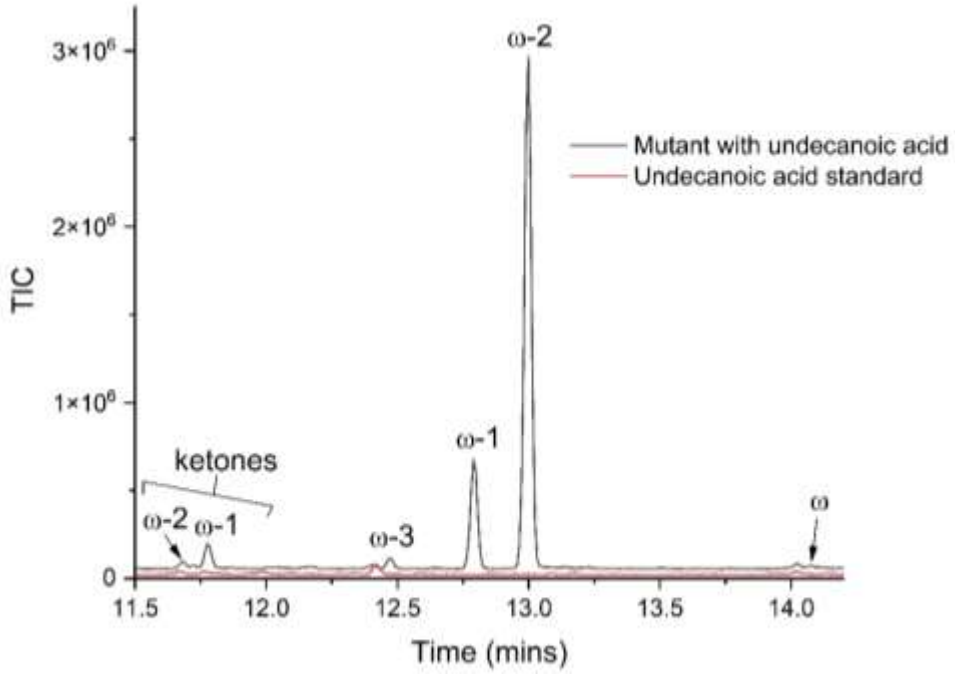

Figure S16 Chromatogram collected from GCMS shows products from H_2O_2 turnovers in the presence of CYP119 GALQEPG, 1 mM undecanoic acid and 50 mM H_2O_2.

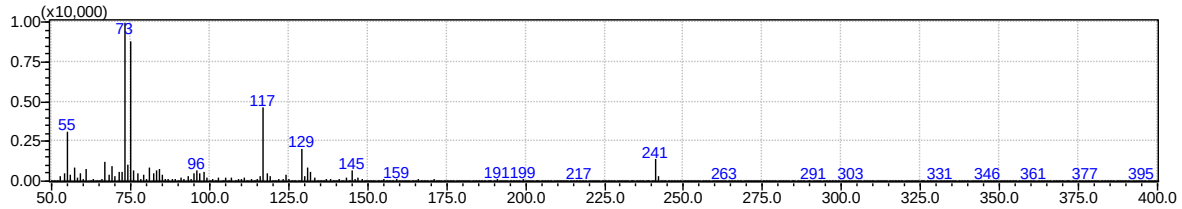

Desaturation of undecanoic acid

10-undecenoic acid. R.T. 8.642 to 8.717**.** Observed m/z = 241 (- 15; -Me) vs expected m/z = 256.

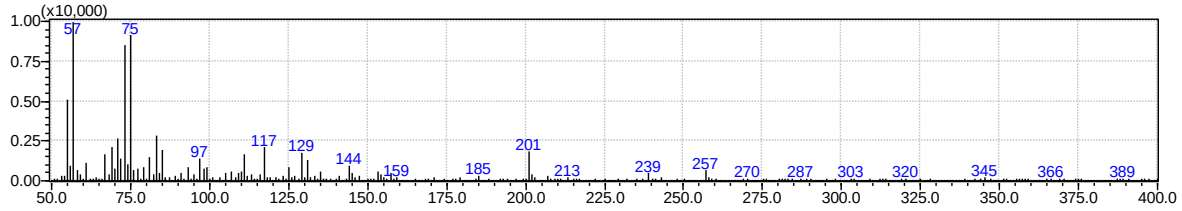

9-oxoundecanoic acid

Undecanoic acid ketone derivative at ω - 2. RT: 11.633 to 11.683. Observed m/z = 257 (- 15; -Me) vs expected 272; fragment at 201.

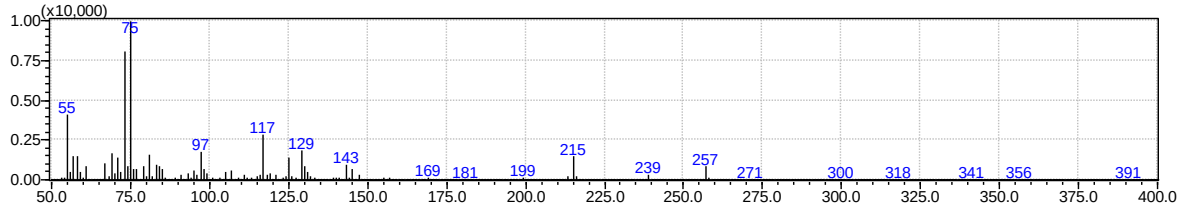

10-oxoundecanoic acid

Undecanoic acid ketone derivative at ω - 1. RT: 11.742 to 11.800. Observed m/z = 257 (- 15; -Me) vs expected 272; fragment at 215.

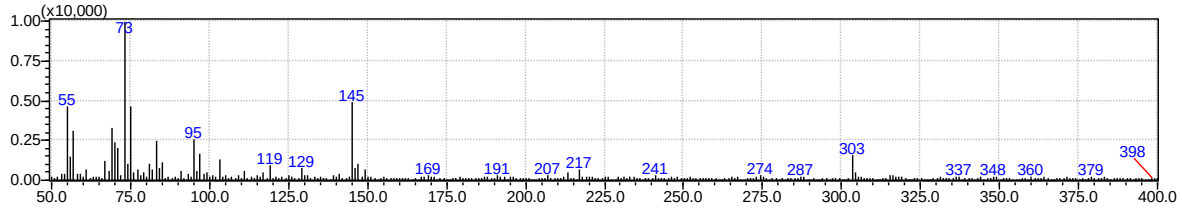

8-hydroxyundecanoic acid

Undecanoic acid hydroxy derivative at ω - 3. RT: 12.367 to 12.433. Observed m/z = 303 (- 43; -C_3H_7) vs expected 346; fragments at 145 and 303.

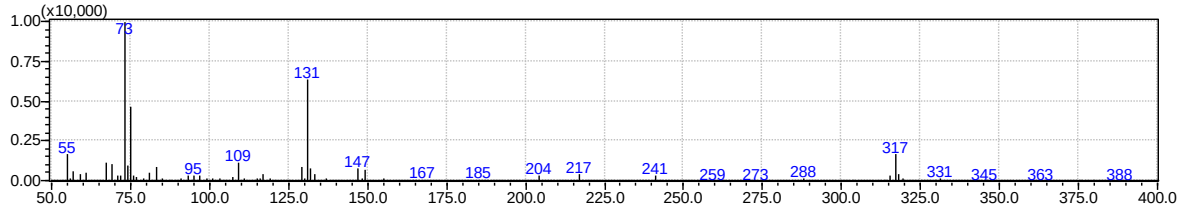

9-hydroxyundecanoic acid

Undecanoic acid hydroxy derivative at ω - 2. RT: 12.750 to 12.808. Observed m/z = 331 (- 15; -Me) vs expected 346; fragments at 131 and 317.

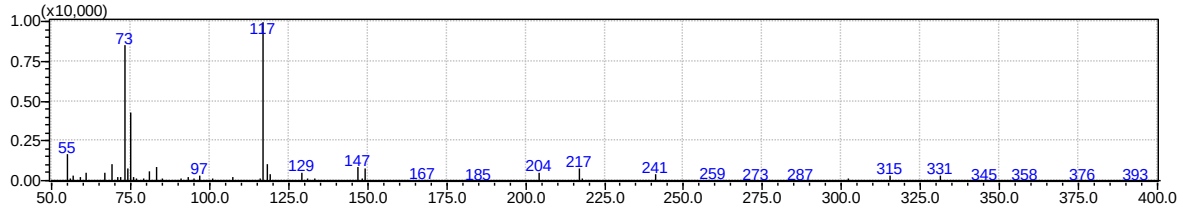

10-hydroxyundecanoic acid

Undecanoic acid hydroxy derivative at ω - 1. RT: 12.950 to 13.025. Observed m/z = 331 (- 15; -Me) vs expected 346; fragments at 117 and 331.

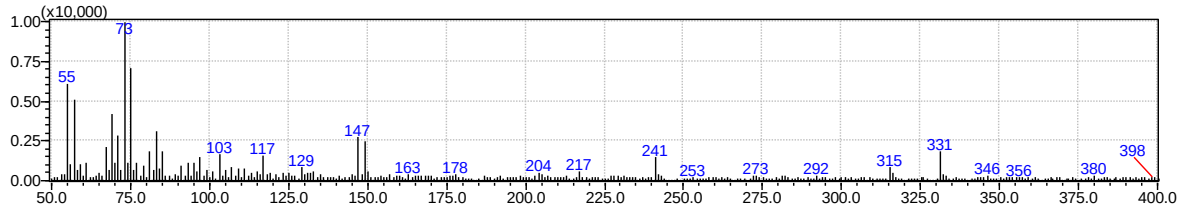

11-hydroxyundecanoic acid

Undecanoic acid hydroxy derivative at ω. RT: 13.992 to 14.033. Observed m/z = 331 (- 15; -Me) vs expected 346; fragment at 103.

Figure S17 Mass spectra associated with chromatogram from Figure S16 for the reaction of undecanoic acid with CYP119 GALQEPG mutant in the presence of H_2O_2.

Tridecanoic acid - C13

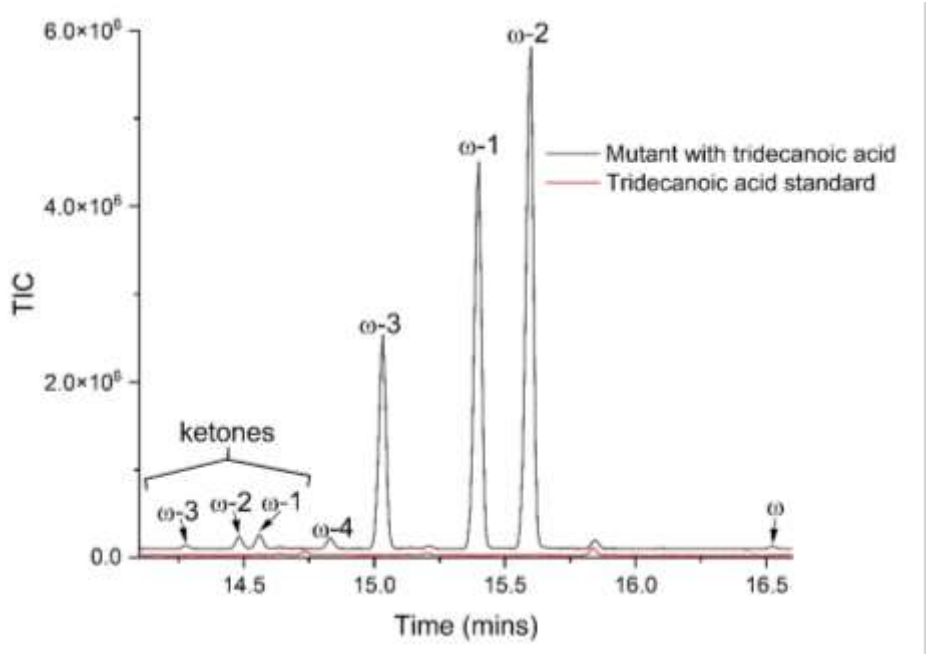

Figure S18 Chromatogram collected from GCMS data shows products from H_2O_2 turnovers in the presence of CYP119 GALQEPG, 1 mM tridecanoic acid and 50 mM H_2O_2.

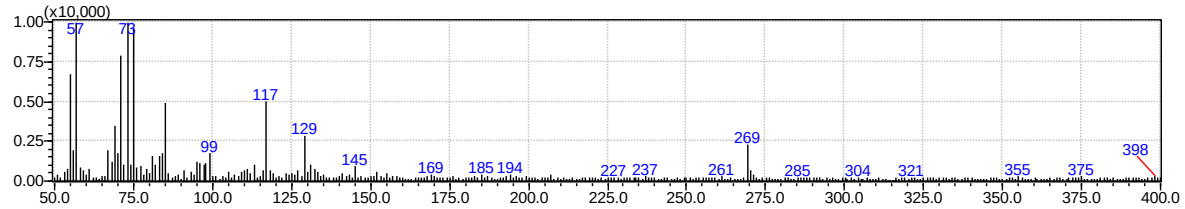

Desaturation of tridecanoic acid

12-tridecenoic acid. R.T. 11.667 to 11.758**.** Observed m/z = 269 (- 15; -Me) vs expected m/z = 284.

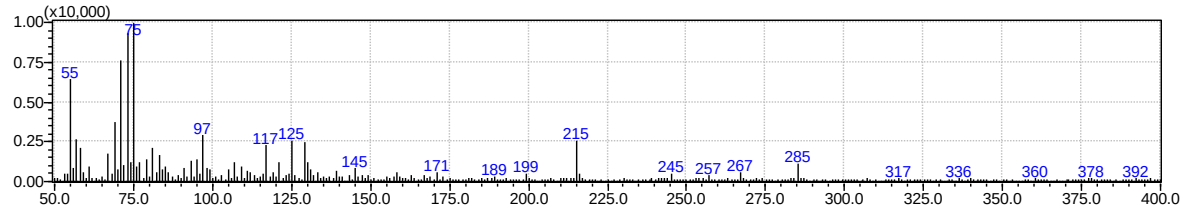

10-oxotridecanoic acid

Tridecanoic acid ketone derivative at ω - 3. RT: 14.258 to 14.292. Observed m/z = 285 (- 15; -Me) vs expected 300; fragment at 215.

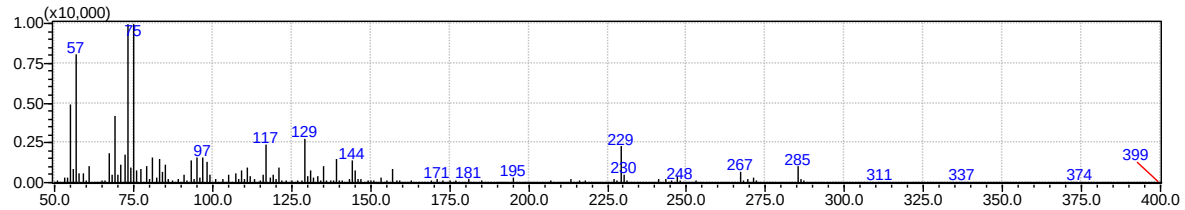

11-oxotridecanoic acid

Tridecanoic acid ketone derivative at ω - 2. RT: 14.450 to 14.508. Observed m/z = 285 (- 15; -Me) vs expected 300; fragment at 229.

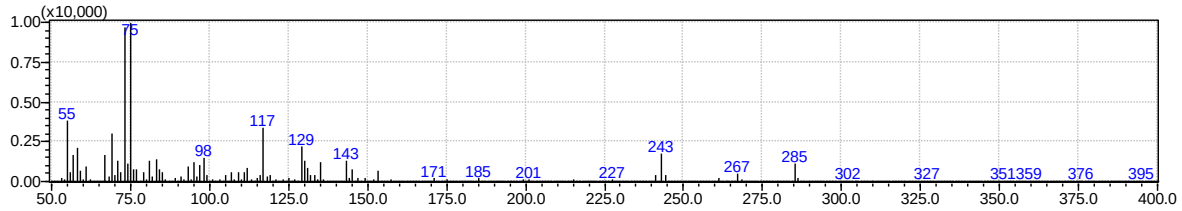

12-oxotridecanoic acid

Tridecanoic acid ketone derivative at ω - 1. RT: 14.525 to 14.592. Observed m/z = 285 (- 15; -Me) vs expected 200; fragment at 243.

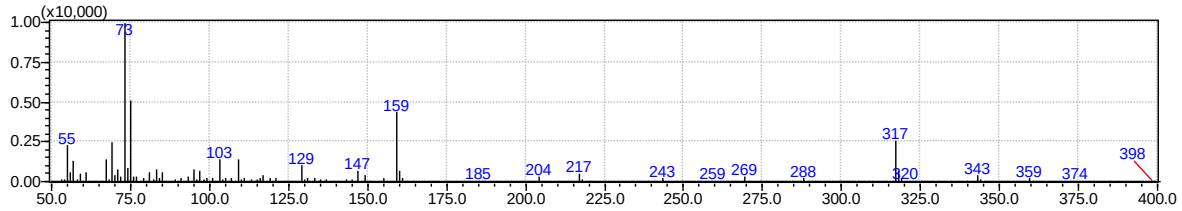

9-hydroxytridecanoic acid

Tridecanoic acid hydroxy derivative at ω - 4. RT: 14.800 to 14.858. Observed m/z =374 and 359 (- 15; -Me) vs expected 374; fragments at 159 and 317.

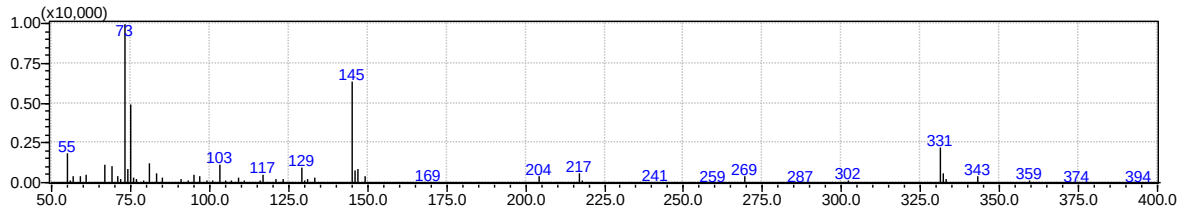

10-hydroxytridecanoic acid

Tridecanoic acid hydroxy derivative at ω - 3. RT: 14.983 to 15.067. Observed m/z =374 and 359 (- 15; -Me) vs expected 374; fragments at 145 and 331.

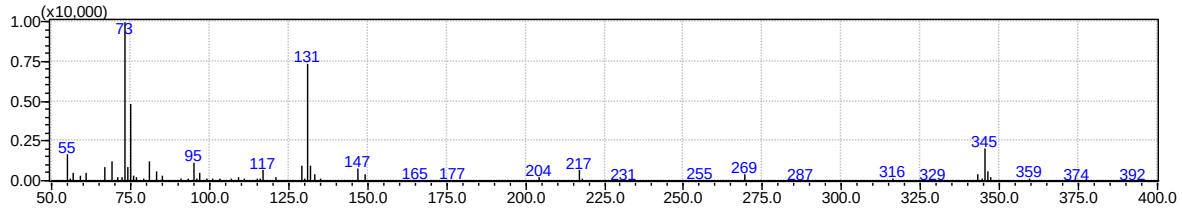

11-hydroxytridecanoic acid

Tridecanoic acid hydroxy derivative at ω - 2. RT: 15.342 to 15.433. Observed m/z =374 and 359 (- 15; -Me) vs expected 374; fragments at 131 and 345.

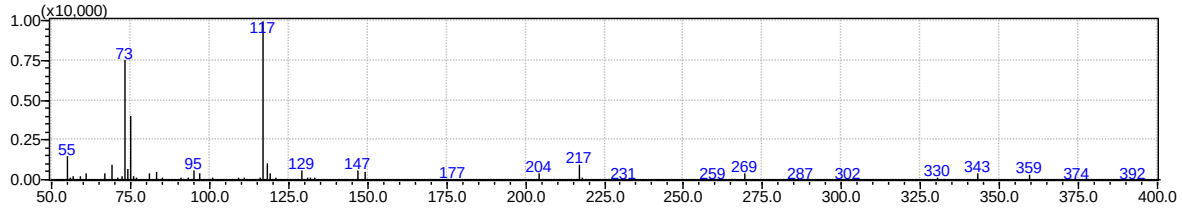

12-hydroxytridecanoic acid

Tridecanoic acid hydroxy derivative at ω - 1. RT: 15.542 to 15.633. Observed m/z =374 and 359 (- 15; -Me) vs expected 374; fragments at 117 and 359.

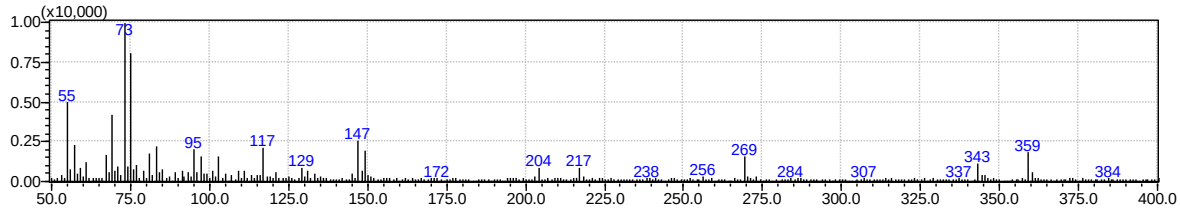

13-hydroxytridecanoic acid

Tridecanoic acid hydroxy derivative at ω. RT: 16.508 to 16.533. Observed m/z = 359 (- 15; -Me) vs expected 374; fragment at 103.

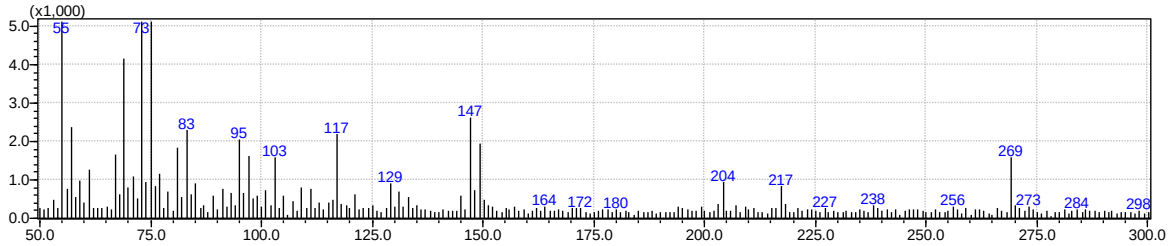

13-hydroxytridecanoic acid

Zoom in to show fragment at 103.

Figure S19 Mass spectra associated with chromatogram from Figure S18 for the reaction of tridecanoic acid with CYP119 GALQEPG mutant in the presence of H_2O_2.

Tetradecanoic acid - C14

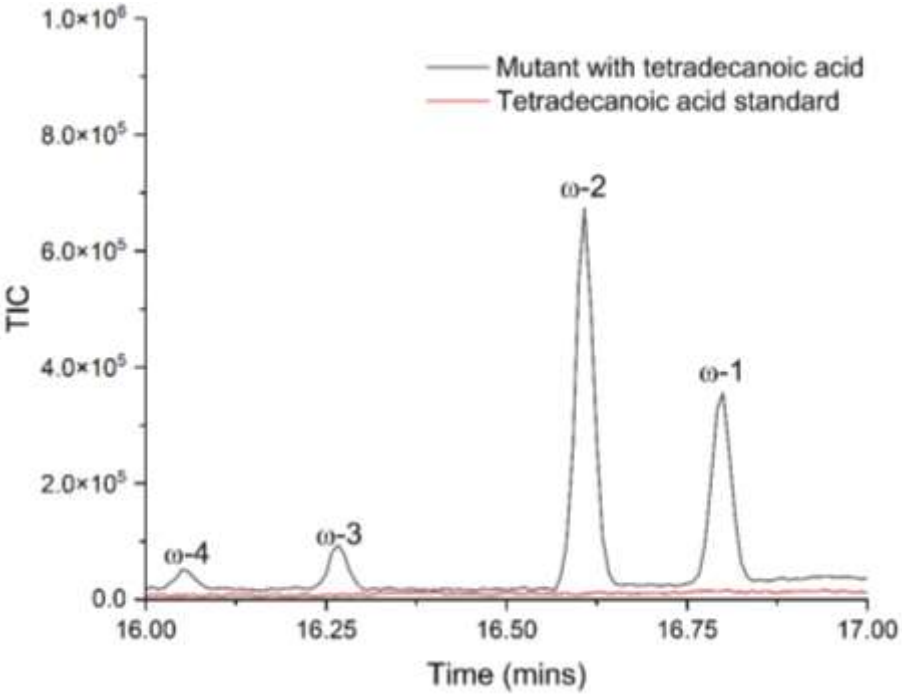

Figure S20 Chromatogram collected from GCMS data shows products from H_2O_2 turnovers in the presence of CYP119 GALQEPG, 1 mM tetradecanoic acid (myristic acid) and 50 mM H_2O_2.

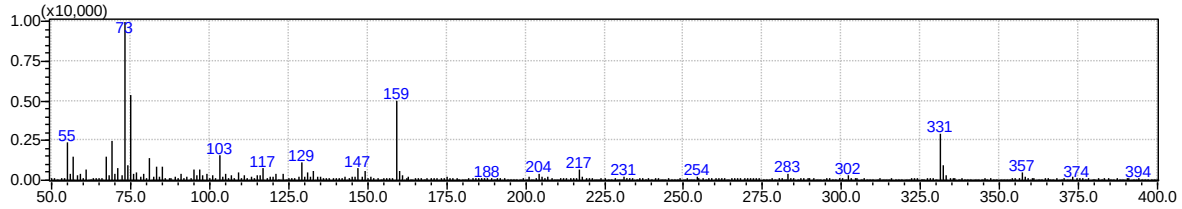

10-hydroxytetradecanoic acid

Tetradecanoic acid hydroxy derivative at ω - 4. RT: 16.033 to 16.067. Observed m/z = 331 (- 57; -C_4H_9) vs expected 388; fragments at 159 and 331.

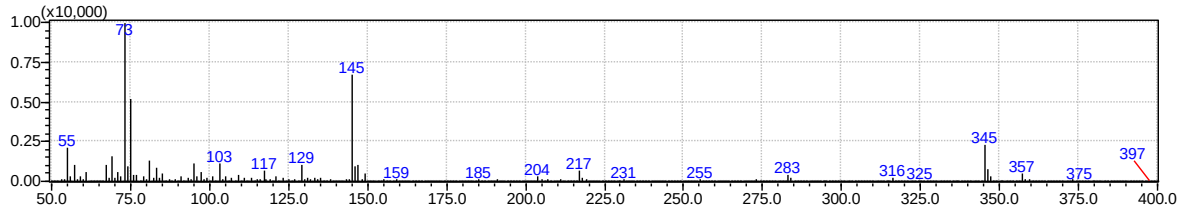

11-hydroxytetradecanoic acid

Tetradecanoic acid hydroxy derivative at ω - 3. RT: 16.242 to 16.283. Observed m/z = 345 (- 43; -C_3H_7) vs expected 388; fragments at 145 and 345.

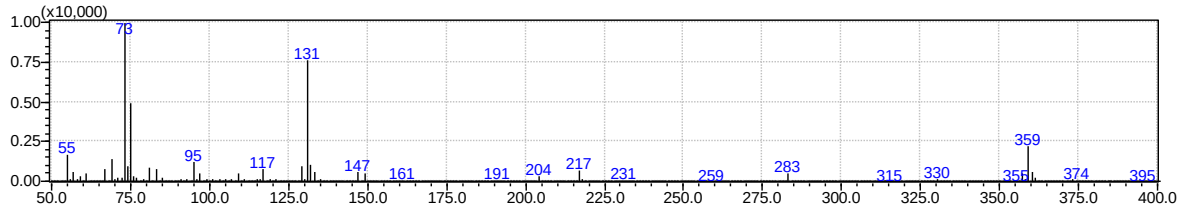

12-hydroxytetradecanoic acid

Tetradecanoic acid hydroxy derivative at ω - 2. RT: 16.575 to 16.633. Observed m/z 357 (- 29; -C_2H_5) vs expected 388; fragments at 131 and 359.

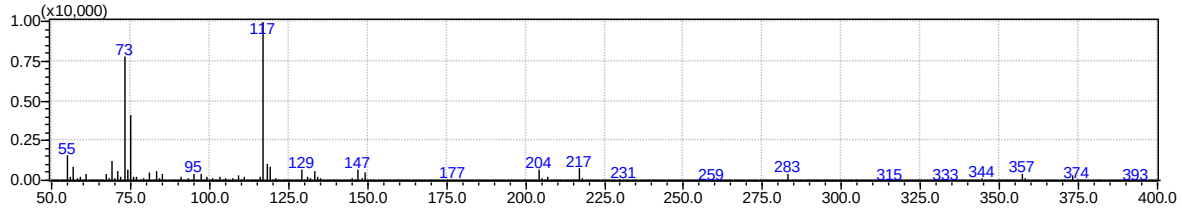

13-hydroxytetradecanoic acid

Tetradecanoic acid hydroxy derivative at ω - 1. RT: 16.767 to 16.833. Observed m/z = 373 (- 15; -Me) vs expected 388; fragments at 117 and 373.

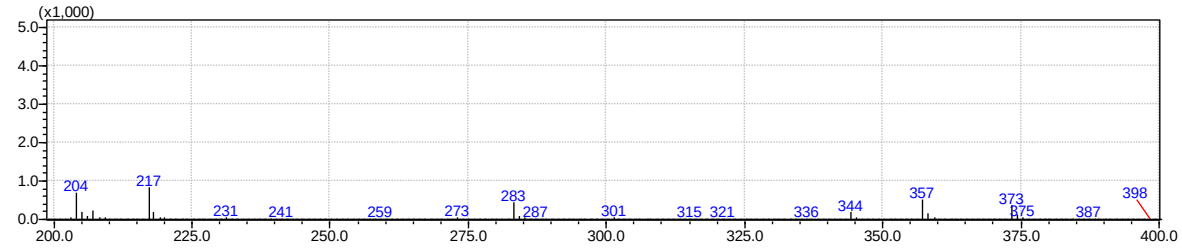

13-hydroxytetradecanoic acid

Zoom in to show fragment at 373.

Figure S21 Mass spectra associated with chromatogram from Figure S20 for the reaction of tetradecanoic acid with CYP119 GALQEPG mutant in the presence of H_2O_2.

[9,9,10,10-d_4]-dodecanoic acid

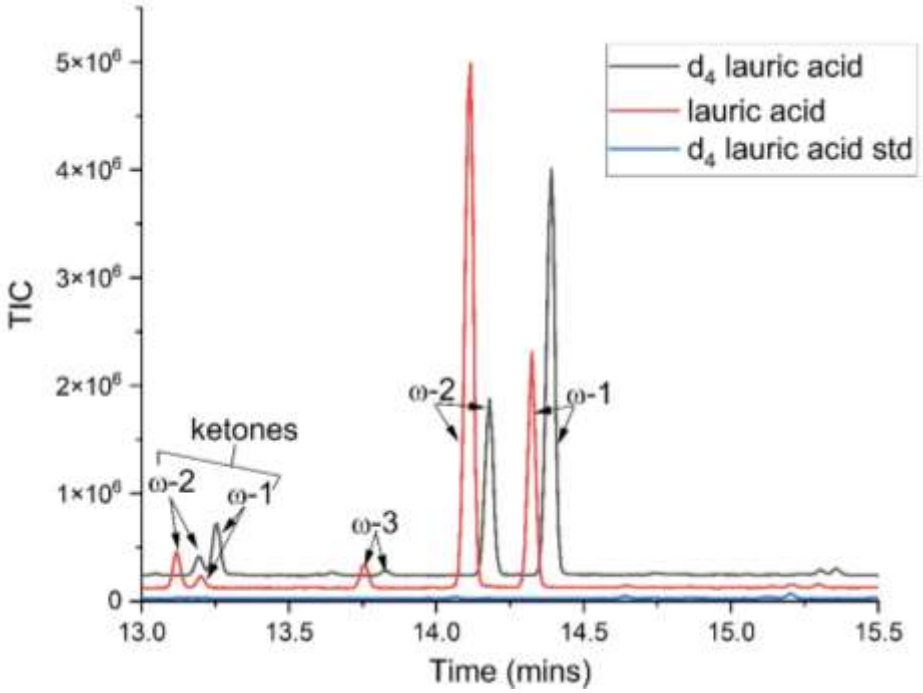

Figure S22 Chromatogram collected from GCMS data shows products from H_2O_2 turnovers in the presence of CYP119 GALQEPG, 1 mM [9,9,10,10-d_4]-dodecanoic acid and 50 mM H_2O_2.

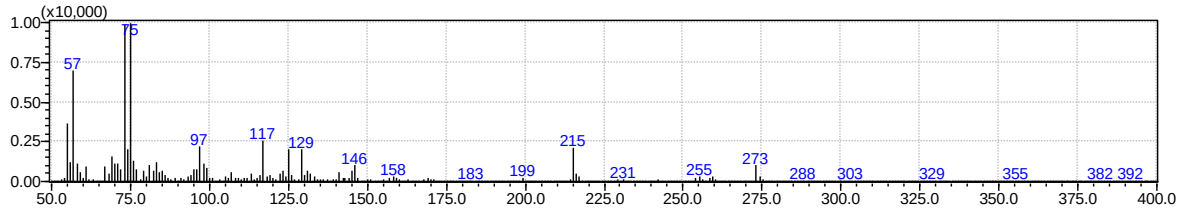

[9,9,10,10-d_4]-10-oxododecanoic acid

[9,9,10,10-d_4]-dodecanoic acid ketone derivative at ω - 2. RT: 13.058 to 13.117. Observed m/z =288 and 273 (- 15; -Me). Expected m/z = 288 versus 286 for non-deuterated species. Fragment at 215; the same as the non-deuterated species.

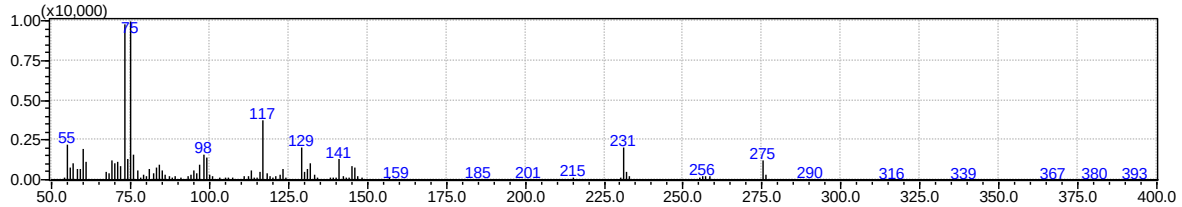

[9,9,10,10-d_4]-11-oxododecanoic acid

[9,9,10,10-d_4]-dodecanoic acid ketone derivative at ω - 1. RT: 13.125 to 13.200. Observed m/z = 290 and 275 (-15; -Me). Expected m/z = 290 versus 286 for non-deuterated lauric acid. Fragment at 231 versus 229 for non-deuterated species.

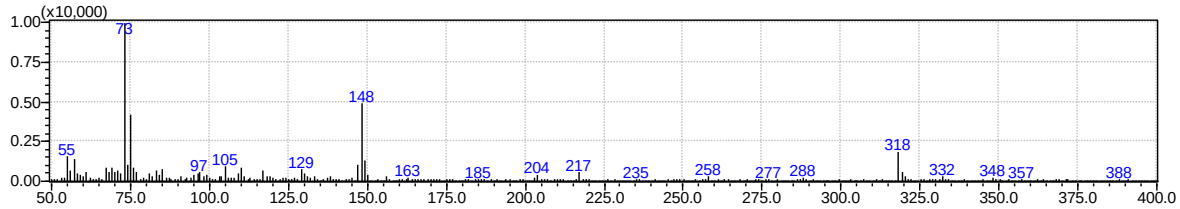

[9,9,10,10-d$_4$]-9-hydroxydodecanoic acid

[9,9,10,10-d$_4$]-dodecanoic acid hydroxy derivative at ω - 3. RT: 13.692 to 13.758. Observed m/z = 348 (- 15; -Me) versus 345 for non-deuterated lauric acid. Expected m/z = 363 versus 360 for non-deuterated lauric acid. Fragments at 148 and 318 versus 145 and 317 for non-deuterated species.

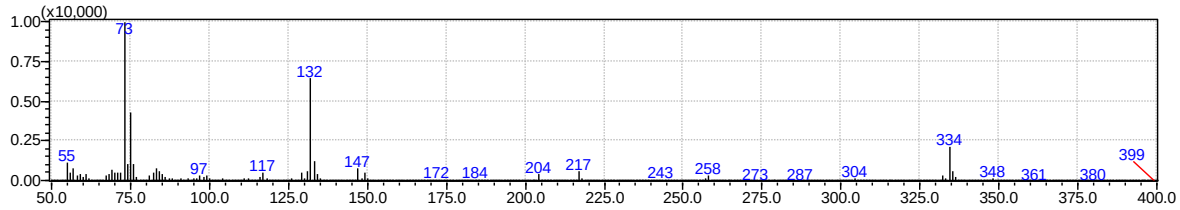

[9,9,10,10-d$_4$]-10-hydroxydodecanoic acid

[9,9,10,10-d$_4$]-dodecanoic acid hydroxy derivative at ω - 2. RT: 14.042 to 14.150. Observed m/z = 348 (- 15; -Me) versus 345 for non-deuterated lauric acid. Expected m/z = 363 versus 360 for non-deuterated lauric acid. Fragments at 132 and 334 versus 132 and 331 for non-deuterated species.

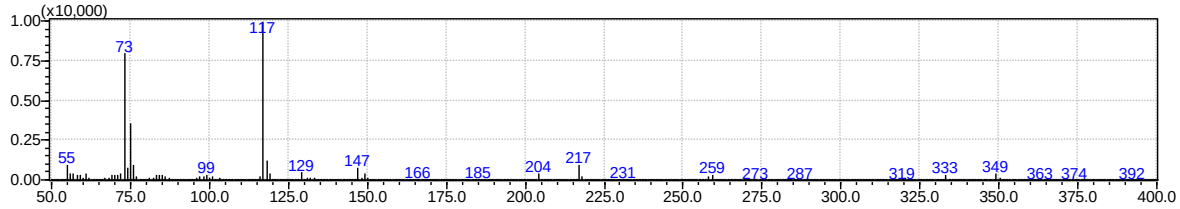

[9,9,10,10-d$_4$]-11-hydroxydodecanoic acid

[9,9,10,10-d$_4$]-dodecanoic acid hydroxy derivative at ω - 1. RT: 14.225 to 14.350. Observed m/z = 349 (- 15, -Me) versus 345 for non-deuterated lauric acid. Expected m/z = 364 versus 360 for non-deuterated lauric acid. Fragments at 117 and 349 versus 117 and 345 for non-deuterated species.

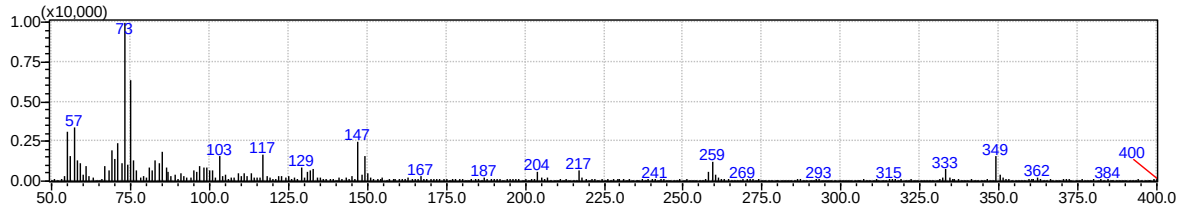

[9,9,10,10-d$_4$]-12-hydroxydodecanoic acid

[9,9,10,10-d$_4$]-dodecanoic acid hydroxy derivative at ω. RT: 15.233 to 15.292. Observed m/z = 349 (- 15, -Me) versus 345 for non-deuterated lauric acid. Expected m/z = 364 versus 360 for non-deuterated lauric acid. Fragments at 103 and 349 versus 103 and 345 for non-deuterated species.

Figure S23 Mass spectra associated with chromatogram from Figure S22 for the reaction of [9,9,10,10-d$_4$]-dodecanoic acid with CYP119 GALQEPG mutant in the presence of H_2O_2.

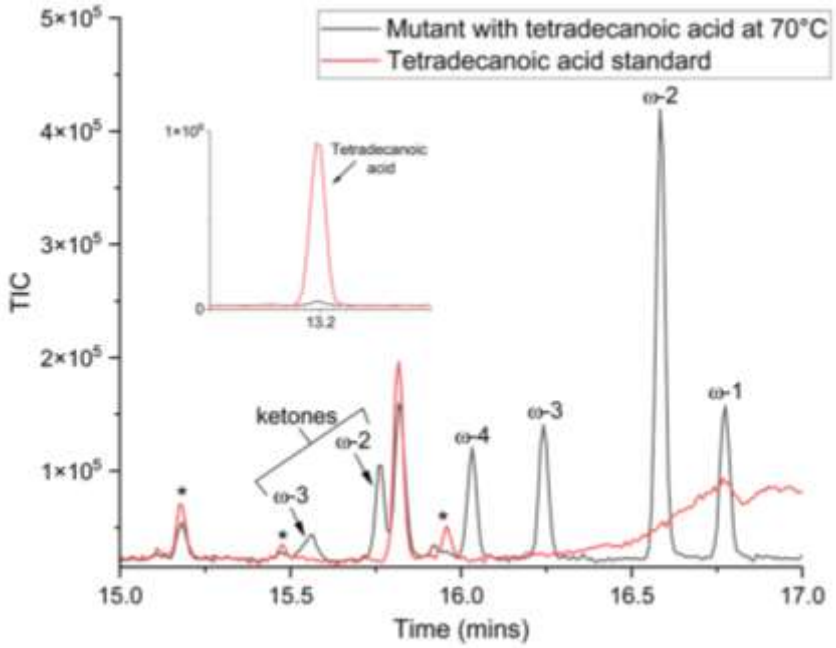

Figure S24 Chromatogram collected from GCMS data shows products from H_2O_2 turnovers in the presence of CYP119 GALQEPG (1 μM), tetradecanoic acid (100 μM; myristic acid) and H_2O_2 (20 mM), reaction time 5 minutes at 70 °C. * denotes the presence of an impurity.[4]

The conditions above were used to compare to those reported previously (5 μM enzyme, 100 μM fatty acid substrate and 20 mM hydrogen peroxide reaction time 1 minute). Our reaction at 70 °C resulted in the almost complete conversion of tetradecanoic acid into metabolites with the generation of some further oxidation metabolites. The rate was 17.9 min^{-1} per equivalent unit of enzyme with total turnover numbers of 90-100 (100 is the maximum available under the reaction conditions). At 30 °C the rate was lower 5.4 min^{-1}. We also did experiments with dodecanoic acid using these conditions (but using a higher concentration of 500 μM as we found it to be a better substrate for the enzyme). The rate of dodecanoic acid oxidation at 70 °C was 19.6 min^{-1}.

The comparable rates of the T213E single enzyme for fatty acid oxidation was 8.3 min^{-1}.[4] (5 μM enzyme, 100 μM fatty acid substrate and 20 mM hydrogen peroxide, maximum total number of turnovers is 20).

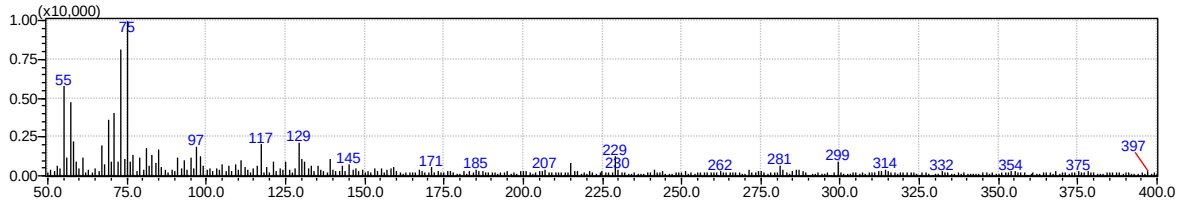

11-oxotetradecanoic acid

Tetradecanoic acid ketone derivative at ω - 3. RT: 15.517 to 15.608. Observed m/z = 314 and 299 (-Me) vs expected 314; fragment at 229.

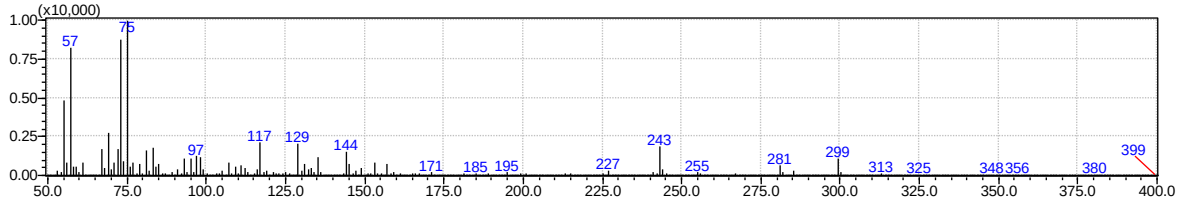

12-oxotetradecanoic acid

Tetradecanoic acid ketone derivative at ω - 2. RT: 15.733 to 15.783. Observed m/z = 299 (-Me) vs expected 314; fragment at 243.

Figure S25 The MS data of ketone metabolites (not generated under other turnover conditions see Figure S20 and S21) with GC chromatogram (Figure S24); reaction of myristic acid with CYP119 GALQEPG in the presence of H_2O_2 under similar conditions previously reported by Shoji *et al.*[4]

References

1. J. Akter, T. P. Stockdale, S. A. Child, J. H. Z. Lee, J. J. De Voss and S. G. Bell, *J. Inorg. Biochem.y*, 2023, **244**, 112209.
2. M. A. McLean, S. A. Maves, K. E. Weiss, S. Krepich and S. G. Sligar, *Biochem Biophys Res Commun*, 1998, **252**, 166-172.
3. F. H. Westheimer, *Chemical Reviews*, 1961, **61**, 265–273.
4. O. Shoji, T. Fujishiro, K. Nishio, Y. Kano, H. Kimoto, S.-C. Chien, H. Onoda, A. Muramatsu, S. Tanaka, A. Hori, H. Sugimoto, Y. Shiro and Y. Watanabe, *Catalysis Science & Technology*, 2016, **6**, 5806–5811.